

## AN ANALYSIS OF TENSILE TEST RESULTS TO ASSESS THE INNOVATION RISK FOR AN ADDITIVE MANUFACTURING TECHNOLOGY

Stanisław Adamczak<sup>1)</sup>, Jerzy Bochnia<sup>1)</sup>, Bożena Kaczmarska<sup>3)</sup>

Kielce University of Technology, Al. 1000-lecia P. P. 7, 25-314 Kielce, Poland,

1) Department of Manufacturing Engineering and Metrology (✉adamj@tu.kielce.pl, +48 22 432 7721)

2) Department of Production Engineering

### Abstract

The aim of this study was to assess the innovation risk for an additive manufacturing process. The analysis was based on the results of static tensile tests obtained for specimens made of photocured resin. The assessment involved analyzing the measurement uncertainty by applying the FMEA method. The structure of the causes and effects of the discrepancies was illustrated using the Ishikawa diagram. The risk priority numbers were calculated. The uncertainty of the tensile test measurement was determined for three printing orientations. The results suggest that the material used to fabricate the tensile specimens shows clear anisotropy of the properties in relation to the printing direction.

Keywords: Failure Mode and Effects Analysis, static tensile test, measurement uncertainty.

© 2015 Polish Academy of Sciences. All rights reserved

### 1. Introduction

Innovative technologies are essential to enhance the competitiveness of business enterprises. However, before a technology is implemented, it needs to be studied in detail. It is necessary to determine all the factors affecting the process, including technical and economic risks. One of the risk assessment tools is the Failure Mode and Effects Analysis (FMEA), commonly used in the aviation, automotive, electronic, chemical and health industries. The applications of the FMEA method are discussed in Ref. [1], which is considered to be an overview of several dozen publications from the period 1992–2012. The paper characterizes the method, its variants and modifications; it also classifies the models and the modifications. Examples of using the FMEA method can be found in the papers concerning the risks of a rotor blade failure in an aero-engine [2], ergonomics of the driver's seat [3] or the risks in the product supply environment [4].

In this study, the FMEA method was used to show schematically the structure of causes and effects by means of the Ishikawa diagram. This type of a diagram is commonly employed to illustrate various measurement problems [5], assess a measurement uncertainty [6], perform a qualitative analysis [7], and assess the manufacture process of machine parts [8].

The FMEA method was applied to assess the innovation risk of the PolyJet additive manufacturing technology. The analysis involved testing the ultimate tensile strength of the photo-cured material, Vero White, and then assessing the uncertainty of the ultimate tensile strength measurements. The specimens were fabricated using different orientations (arrangements on the build tray). The measurement results were used to assess the risk priority numbers by means of the FMEA methodology.

Assessing the innovation risk associated with additive manufacturing technologies is vital because of their dynamic development and application in many areas of engineering, ranging

from various industries through design, architecture to medicine. They are becoming popular to construct not only models or prototypes, but also finished or semi-finished products. The present state of knowledge and future potential of additive manufacturing technologies are discussed, for example, by Campbell [9]. He analyzes their industrial applications, advances in materials and design trends.

The materials used in additive manufacturing are:

- liquids, e.g. a photo-cured resin for the PolyJet technology,
- powders (loose media), e.g. a polyamide powder for Selective Laser Sintering (SLS) or a ceramic powder for 3D Printing,
- solids (wire, foil), e.g. an ABS wire for Fused Deposition Modelling (FDM).

The finished object fabricated on the build tray of a 3D printer is a solid with properties considerably different from those of the semi-finished product. The mechanical properties of the material used are modelled during the manufacturing (printing) process. Thorough investigations are necessary to study the properties of these new, innovative materials.

Advances in the technology of materials for additive manufacturing, including the development of new materials with better physical and mechanical properties, require a detailed analysis of these properties. For example, Ref. [10] is an interesting source of information about the effects of the environment (aging) and the printing orientation (i.e. an arrangement on the build tray) on mechanical properties of the produced objects. Reference [11] discusses how the direction of the layer deposition and the process of laser sintering of polyamide powders influence mechanical properties of these objects. Some of the papers concerned with an analysis of the mechanical properties of materials fabricated by additive manufacturing [12–14] also point to the material anisotropy in relation to the object orientation on the printer build tray.

## 2. Assessment of innovation risk vs. measurement uncertainty

The term “risk” is related to a likelihood of occurring undesired events or conditions. The numerical value of the risk can be the probability of their occurrence. The risk associated with an innovative process can be high, because the knowledge about the process does not result from an experience. In such cases, there exists a considerable uncertainty related to the process and the achieved objectives. The uncertainty can be reduced through procedures called the risk management, comprising the risk analysis, understood as an analysis of causes and effects of occurring unfavourable events. The analysis shows what preventive measures should be taken. The risk analysis is a crucial process, especially if the research results are to be implemented. The risk analysis should be performed periodically using the experience gained during research, so that the risk data and the risk response methods are up-to-date and that they can be used, for example, in tensile testing, a surface texture analysis, as well as testing engines [15, 16] or industrial control systems [17].

A classical analysis of measurement results includes assessing an uncertainty, characterizing the scatter of results, with the results being appropriately attributed to the measured quantities. However, the analysis does not refer to the process of fabricating the measured product; it does not involve analysing and assessing the causes and effects of the discrepancies reported during the measurement. There is no analysis allowing to identify the risk and, if possible, eliminate or at least reduce it.

The *Failure Mode and Effects Analysis* (FMEA) is a well-known and common method for analysing and assessing the measurement results, and - accordingly - risks. It is applied in a number of engineering areas for the risk prevention in the quality management. It allows to obtain an additional information, including causes and effects of the discrepancies identified

during the measurement process, taking into account a severity of the measurement uncertainty, which is represented graphically in Fig. 1.

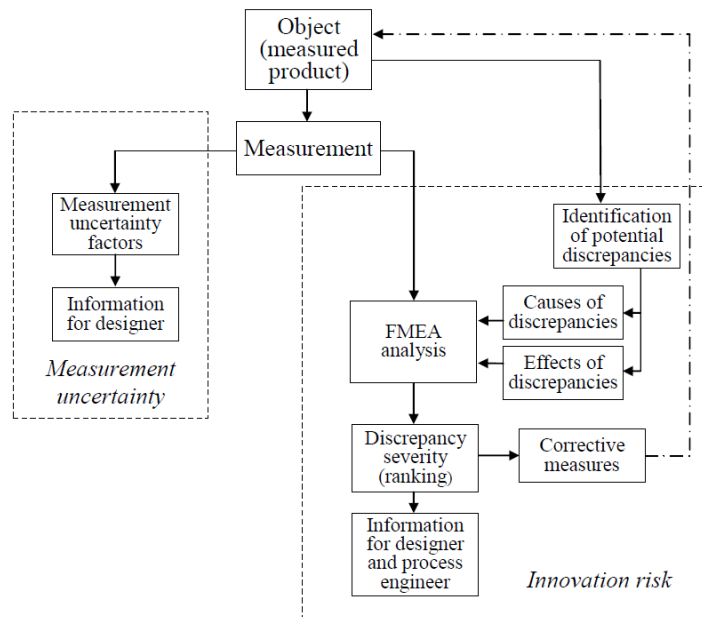


Fig. 1. The FMEA method employed to analyze the measurement uncertainty.

The FMEA method is used to study the potential or real discrepancies (or failures). On the basis of the causes and effects, it determines the severity of each discrepancy, whose measure, from the quantitative point of view, is the risk priority number (P) calculated as a product of three factors.

$$P = Z \cdot R \cdot W, \quad (1)$$

Z – the severity expressed by unfavourable effects of the discrepancies during the product use;  
 R – the risk understood as the probability (frequency) of occurring discrepancies during the manufacturing process;

W – the detectability, determined as a difficulty to show the discrepancies before the product use.

The values of these factors are calculated on the basis of the information about the process and the product or on the basis of specially performed tests. In a classical approach to the method, the values of the factors range between 1 and 10; hence, the risk priority number assumes values from the range (1 – 1000). When the discrepancies are ranked according to their severity, it is easier to develop a plan of corrective measures, being part of the innovation risk management.

In this study, the factors were determined by performing an innovation risk analysis, which involved assessing the measurement uncertainty of the ultimate tensile strength for specimens produced by additive manufacturing using a photo-cured material. The description of the specimen preparation and the static tensile testing as well as the analysis of results are included in the next sections.

### 3. Materials and methods

The specimens were made of a photo-cured resin, Vero White, by means of an Objet Connex 350 3D printer based on the PolyJet technology (<http://objet.com/3d-printing->

materials). The specimens were produced in accordance with ISO 527-1 [18], with dimensions being as follows: the narrow section width -  $5\pm 0.05$  mm; the narrow section length -  $30\pm 0.05$  mm; the nominal thickness - 4 mm (recommended by the standard  $\geq 2$  mm); the grip section width -  $10\pm 0.5$  mm; and the overall length  $\geq 75$  mm.

A solid 3D model of a specimen was created in a CAD program and saved as an *.stl* file. The triangulation parameters which are to be exported include: the resolution – adjusted, the deviation – a 0.016 mm tolerance, and the angle – a  $5^\circ$  tolerance. It is crucial that the values of the triangulation parameters should not be too low to ensure rounded edges (in this case, the fillet radius between the grip section and the gauge section); they should not be too high, either, so as not to increase the volume of the file (*\*.stl*).

Subsequently, the specimen models were virtually placed on the build tray of the Connex 350 printer (the net build size:  $255 \times 252 \times 200$  mm) using the Objet Studio program. The specimen models were arranged in three different orientations:

- in the X-direction – along the longitudinal movement of the print-head, with one side of the model touching the build tray,
- in the Y-direction – along the longitudinal movement of the print-head, with the flat side of the model touching the build tray,
- in the Z-direction – with the specimen placed vertically.

The specimens were produced in the Glossy mode to ensure a smooth surface. In this mode, the support material is added only as the bed or to fill in the missing details; the other surfaces remain smooth. Figure 2 shows the virtual arrangement of the specimen models over the build tray in the Objet Studio program. Vertically arranged specimens were printed in batches, as shown in Fig. 2. The distance between two adjacent specimens was 2 mm and the space between them was filled with the support material. This caused the specimens to stick together and guaranteed the printing stability in the vertical direction. When a single vertically oriented specimen is produced, it may collapse after a certain height is reached. The layer thickness was 0.016 mm.

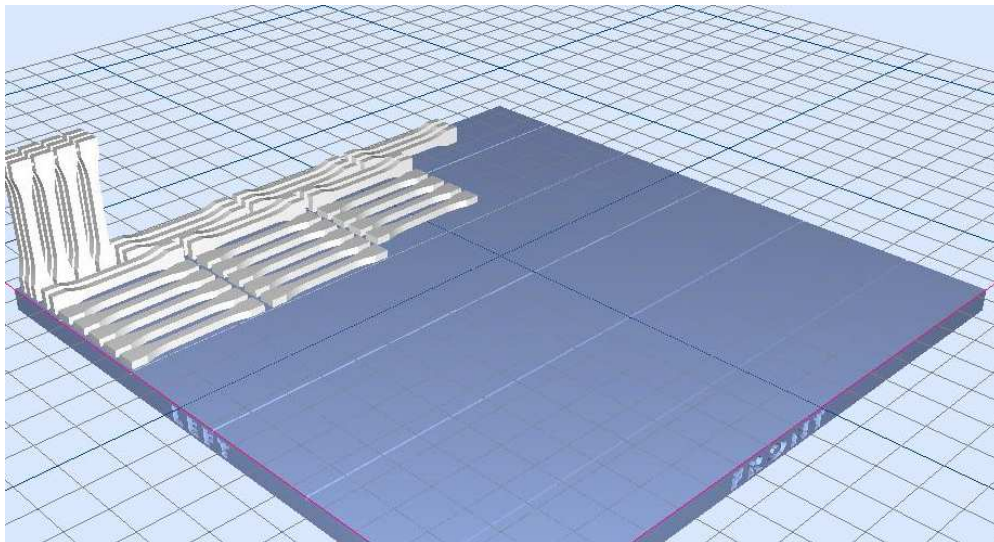


Fig. 2. Specimen models on the build tray in the Objet Studio program.

After removing the printed specimens and the support material off the build tray, the specimens were prepared for static tensile tests. The testing was performed using an Inspekt mini universal testing machine [19] and an extensometer to measure deformations. The test speed was set at 1 mm/min in the LabMaster program [20] that the Inspekt mini universal

testing machine is equipped with. The tensile tests were performed for the total of 30 specimens. Each printing orientation was represented by 10 specimens. This number was assumed to be sufficient, as proved in Ref. [21], where the tensile tests and assessing the uncertainty of results were performed for a series of 30 specimens.

#### 4. Results and discussion

The exemplary plots in Fig. 3 show the stress-strain relationships drawn by a computer connected to the universal testing machine.

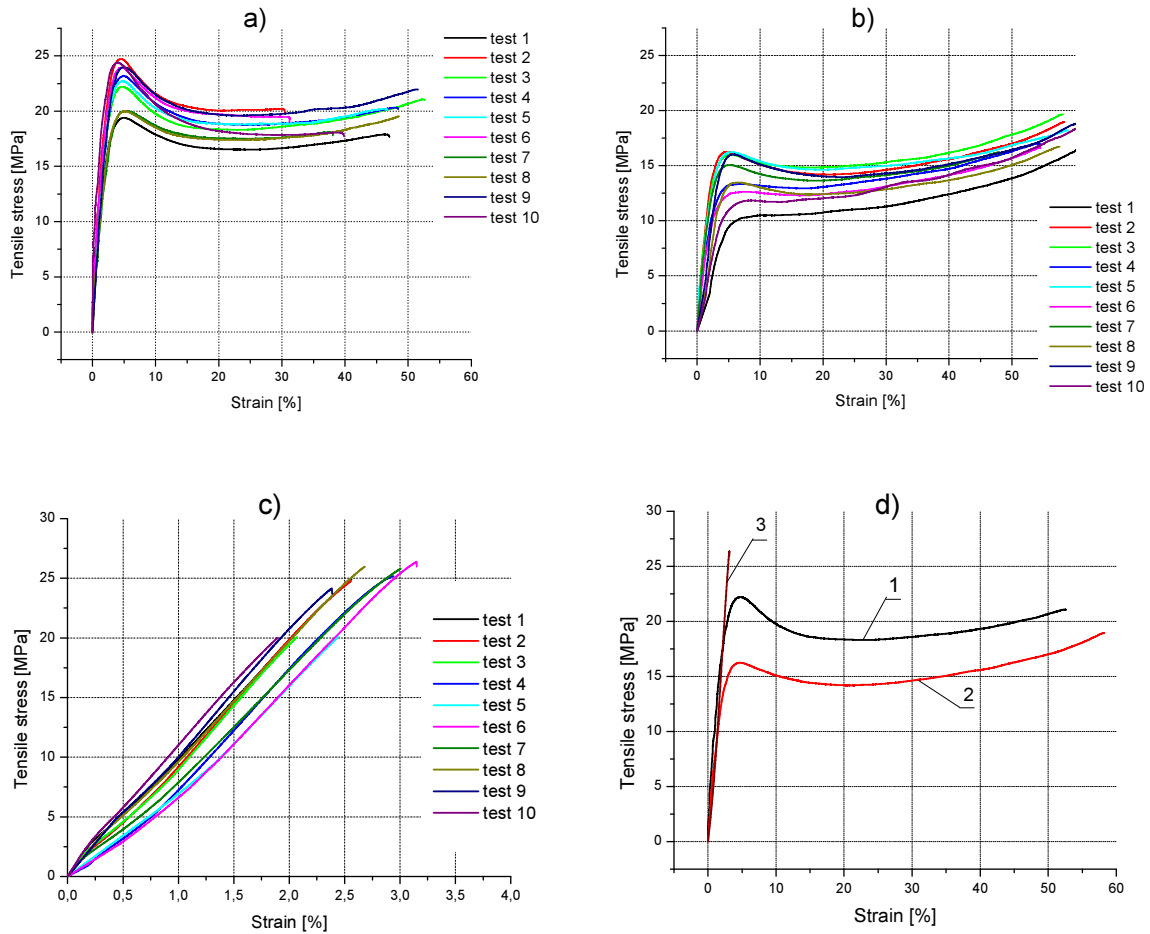


Fig. 3. Tensile test plots for specimens:

- a) placed on the side and oriented in the X-direction, along the longitudinal movement of the print-head;
- b) placed on the flat side and oriented in the Y-direction, along the longitudinal movement of the print-head;
- c) oriented vertically in the Z-direction;
- d) selected from each series: 1- oriented in the X-direction, 2 - oriented in the Y-direction, 3 - oriented vertically in the Z-direction.

Table 1 contains: values of the maximum tensile load  $F_m$  for specimens oriented in the X, Y, and Z-direction and the average value of the maximum tensile force calculated for each printing direction, which are needed to calculate the measurement uncertainty.

Table 1. Values of the maximum tensile load  $F_m$  for specimens oriented in the X-direction, Y-direction and Z-direction.

Test number	X-direction Maximum load $F_{mi}$ [N]	X-direction $(F_{mi} - \bar{F}_m)^2$ [N <sup>2</sup> ]	Y-direction Maximum load $F_{mi}$ [N]	Y-direction $(F_{mi} - \bar{F}_m)^2$ [N <sup>2</sup> ]	Z-direction Maximum load $F_{mi}$ [N]	Z-direction $(F_{mi} - \bar{F}_m)^2$ [N <sup>2</sup> ]
1	2	3	4	5	6	7
Test 1	392.6	4116.51	366.8	10.76	558.2	700.66
Test 2	500.7	1930.72	385.5	483.12	559.0	743.65
Test 3	450.3	4173.16	398.3	1209.65	451.6	6420.82
Test 4	470.7	194.32	342.3	450.29	567.9	1308.27
Test 5	461.6	23.41	368.2	21.90	456.1	5719.90
Test 6	486.4	878.51	334.9	819.10	588.9	3268.41
Test 7	403.7	2815.36	326.9	1341.02	579.4	2272.43
Test 8	419.2	1410.75	355.7	61.15	578.8	2215.59
Test 9	487.0	914.46	379.4	252.17	539.8	65.13
Test 10	495.4	1493.05	377.2	187.14	437.6	8860.46
$\bar{X}$	<b>456.76</b>		<b>363.52</b>		<b>531.73</b>	
$\Sigma$		<b>13818.86</b>		<b>4836.32</b>		<b>31575.30</b>

The Labmaster program calculated the ultimate tensile strength,  $R_m$ , using the specimen width and thickness, and the maximum tensile load. The average values of the ultimate tensile strength are, respectively:

- $\bar{R}_{mx} = 22.6$  MPa – for specimens printed in the X-direction,
- $\bar{R}_{my} = 17.9$  MPa – for specimens printed in the Y-direction,
- $\bar{R}_{mz} = 23.7$  MPa – for specimens printed in the Z-direction.

The standard measurement uncertainty of the ultimate tensile strength  $R_m$  for specimens produced in different orientations was calculated using the type-A evaluation from the formula [22]:

$$u_{\bar{y}} = \sqrt{\sum_{i=1}^n \left( \frac{\partial y}{\partial x_i} \right)^2 \cdot u_i^2}, \quad (2)$$

where:  $u_i$  – standard measurement uncertainty of the input data calculated using the type-A or type-B evaluation.

The standard measurement uncertainty of the maximum load  $F_m$  for specimens produced in different orientations was calculated using the type-A evaluation from the formula [22]:

$$u_A = \sqrt{\frac{1}{n(n-1)} \sum_{i=1}^n (x_i - \bar{x})^2}, \quad (3)$$

where:  $n$  – the number of measurements,

$\bar{x}$  – the arithmetic mean of all quantities measured in a series.

The standard measurement uncertainty of the specimen width and thickness was calculated using the type-B evaluation from the formula [23]:

$$u_B = \frac{a}{\sqrt{3}}, \quad (4)$$

where:  $a$  – half of the width of the interval containing a boundary error.

The uncertainty of the average value of the ultimate tensile strength was calculated using the formula (3), and it depended on the printing orientation:

- $u_{F_m} = 12.39$  N – for specimens printed in the X-direction,
- $u_{F_m} = 7.33$  N – for specimens printed in the Y-direction,
- $u_{F_m} = 18.73$  N – for specimens printed in the Z-direction.

The specimen width,  $b_0$ , was measured with an accuracy of 0.05 mm, whereas the thickness  $a_0$  was measured with an accuracy of 0.01 mm, following the recommendations of [15]. The average values were:

- the thickness  $\bar{a}_0 = 4.03$  mm, the width  $\bar{b}_0 = 5.03$  mm, for the X-direction,
- the thickness  $\bar{a}_0 = 4.02$  mm, the width  $\bar{b}_0 = 5.05$  mm, for the Y-direction,
- the thickness  $\bar{a}_0 = 4.2$  mm, the width  $\bar{b}_0 = 5.33$  mm, for the Z-direction.

As there was a very small statistical scatter of results, the measurement uncertainty was not determined using the type-A evaluation. The standard uncertainty determined with formula (4) using the type-B evaluation was:

- for the specimen thickness  $u_{aB} = 0.0029$  mm,
- for the specimen width  $u_{bB} = 0.014$  mm.

The uncertainty of the ultimate tensile strength  $R_m$  values was calculated using the transformed formula (2):

$$u_{R_m} = \sqrt{\left(\frac{1}{\bar{a}_0 \bar{b}_0}\right)^2 u_{F_m}^2 + \left(\frac{-\bar{F}_m}{\bar{a}_0^2 \bar{b}_0}\right)^2 u_{aB}^2 + \left(\frac{-\bar{F}_m}{\bar{a}_0 \bar{b}_0^2}\right)^2 u_{bB}^2}, \quad (5)$$

where:  $\bar{F}_m$  – the average value of the maximum tensile force calculated for each printing direction (Tables 1),

$u_{F_m}$  – the uncertainty of the average value of the maximum tensile force,

$\bar{a}_0$  – the average thickness of the specimens,

$u_{aB}$  – the uncertainty of the average thickness of the specimens,

$\bar{b}_0$  – the average width of the specimens,

$u_{bB}$  – the uncertainty of the average width of the specimens.

The values calculated with the formulae (3 and 4), presented in Table 1, were inserted into the formula (5) to determine the measurement uncertainty of the ultimate tensile strength for different arrangements of specimens on the build tray:

- for the specimens printed in the X-direction  $u_A = 0.615$  MPa.
- for the specimens printed in the Y-direction  $u_A = 0.365$  MPa.
- for the specimens printed in the Z-direction  $u_A = 0.839$  MPa.

From the analysis it is evident that the specimens differently arranged on the build tray vary not only in the values of their parameters, e.g. values of the ultimate tensile strength, but can also be classified into different classes of polymers. The following are assumptions made using, for example, the ISO-527 standard:

- the material of the specimens printed in the X-direction (with the side touching the build tray) was classified as a reinforced polymer with no yield point,
- the material of the specimens printed in the Y-direction (with the flat side touching the build tray) was classified as a reinforced polymer with a yield point,
- the material of the specimens printed in the Z-direction (placed vertically) was classified as a brittle polymer.

It should be noted that, chemically, in each case, it is the same material, with its commercial name Vero White. However, the different methods of specimen fabrications, i.e. the different directions of layer depositions, and, accordingly, the different directions of HV photo-curing, cause that the produced solids have different material properties.

Moreover, the analysis results show that the tensile strength  $R_m$  of the specimens placed vertically is 4.6 % higher than that of the specimens fabricated in the X-direction and 24.47 % higher than the strength of the specimens produced in the Y-direction. It is surprising that there is no typical plastic deformation, as illustrated in Fig. 5.

The highest measurement uncertainty of the ultimate tensile strength was reported for the specimens printed in the Z-direction. It was 26 % and 56 % higher than that obtained for the specimens printed in the X- and Y-directions, respectively.

The results suggest that there is clear anisotropy of the material properties, dependent on the printing direction.

The determination of the strength properties and the evaluation of the uncertainty of results are crucial both in engineering calculations and in the assessment of the innovation risks associated with the implementation of new technologies.

### 5. Risk assessment using the FMEA method and measurement results

In the case of products made by additive manufacturing (3D printing), discrepancies may occur at three stages: the design, the process and the measurement. When focus is on the geometry and the strength, five groups of causes of discrepancies can be distinguished. Hence, there are geometrical discrepancies and strength (physical) discrepancies, which affect the product use. The structure of causes and effects of these discrepancies is shown schematically using the Ishikawa diagram (Fig. 4).

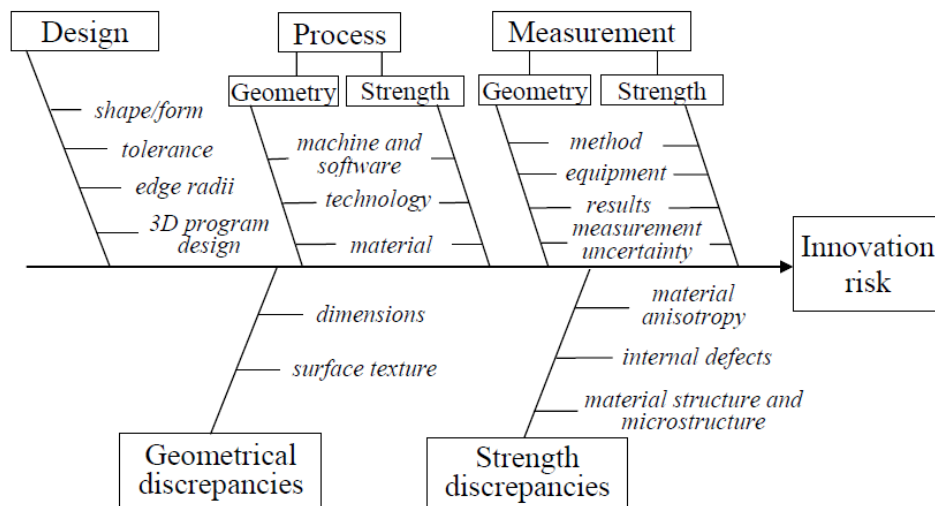


Fig. 4. The Ishikawa diagram – the causes and effects.

As suggested in the FMEA method, the values of the Z, R and W factors were estimated on the basis of the knowledge of the additive manufacturing methods and the experience in the engineering design. For each factor, five levels of the rating scale of the assessed property were assumed. They are presented with the numerical values in Table 2, which was developed on the basis of Ref. [24].

Table 2. The FMEA factors.

Severity		Frequency of occurrence			Detectability	
Rating Scale	Z	Rating Scale	Risk	R	Rating Scale	W
Very low	1-2	Very low	0.00002	1-2	Very high	1-2
Low	3-4	Low	0.0002	3-4	High	3-4
Moderate	5-6	Moderate	0.002	5-6	Moderate	5-6
High	7-8	High	0.02	7-8	Low	7-8
Very high	9-10	Very high	0.2	9-10	Very low	9-10

The factors were determined for seven elements of the process marked in the Ishikawa diagram as five causes and two effects of the occurrence of discrepancies. Using the knowledge of the additive manufacturing methods and the experience in the engineering design, it was possible to estimate the values of the factors and determine the values of the risk priority number (Table 2). The results were represented graphically in Fig. 5.

- Design: it was assumed that a correct design would have a close-to-high severity ( $Z = 6$ ). In the case of innovative solutions, discrepancies occur relatively frequently ( $R = 6$ ), yet they are easy to detect ( $W = 2$ ) through the verification and validation.
- Process – geometry: geometrical discrepancies occurring during the manufacturing process may have low values (by percentage) and a little effect on the product properties ( $Z = 3$ ); since a high quality equipment was used, the probability of occurrence was low ( $R = 3$ ); the detectability was high because of the capabilities of the measurement equipment ( $W = 2$ ).
- Process – strength: the tensile test results obtained for the specimens produced by additive manufacturing from a photo-cured material described in this paper indicate clearly the occurrence of an anisotropy of the material properties, which is attributable to the printing orientation; large discrepancies may affect the quality of products. The severity of strength properties is close to high ( $Z = 6$ ); as a high-quality equipment was used, the probability of occurring discrepancies was moderate ( $R = 5$ ), and the detectability prior to destructive testing was low ( $W = 7$ ).
- Measurement – geometry: a measurement accuracy of geometrical parameters is very significant for the strength analysis ( $Z = 7$ ); for the equipment used, the probability of occurring an error was very low ( $R = 2$ ) and an error was easy to detect because of the procedures assuming the measurement repeatability ( $W = 2$ ).
- Measurement – strength: the severity of the measurement reliability was high ( $Z = 7$ ), because the equipment used was of a high quality; the risk of occurring an error was low ( $R = 3$ ). However, in the case of destructive testing, the detectability of a defect is low ( $W = 6$ ).
- Geometrical discrepancies: the severity of proper dimensioning is high ( $Z = 7$ ). The measurements of the shape of the specimens used for tensile testing show small statistical errors (small scatters of results in the measurement series). The measurement uncertainty for the specimen width and thickness was determined using the type-B evaluation. On average, the probability of occurring this type of discrepancies was low ( $R = 4$ ), and the detectability was high ( $W = 2$ ).
- Strength discrepancies: the severity of strength properties was assumed to be high ( $Z = 7$ ). High values of the strength discrepancies resulting from an anisotropy of the photo-cured material modelled by additive manufacturing indicate an uncertainty of the tensile test measurements for a given printing orientation. For instance, for the orientation in the Z-direction, it was 0.839 MPa. The probability of occurring this type of discrepancies ( $R = 5$ ) was moderate, because high-quality printers were used to produce the elements. The detectability was low ( $W = 7$ ), because of the use of destructive testing.

Table 3. Discrepancies and their values.

Discrepancies	Factors			
	Z	R	W	P
Design	6	6	2	72
Process - geometry	3	3	2	18
Process - strength	6	5	7	210
Measurement - geometry	7	2	2	28
Measurement - strength	7	3	6	126
Geometrical discrepancies	7	4	2	56
Strength discrepancies	7	5	7	245

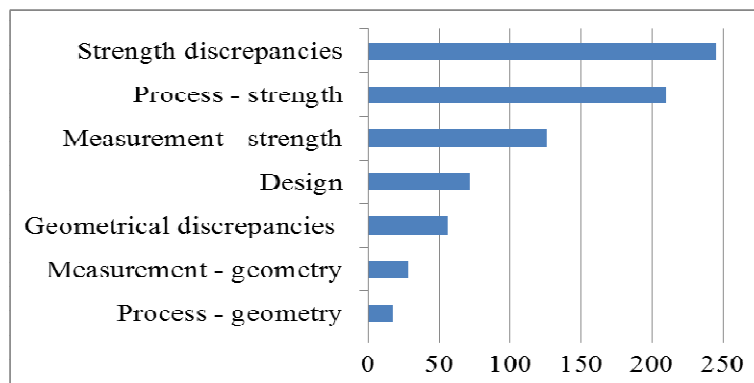


Fig. 5. The risk priority number.

There are three important discrepancies related to the strength properties of products. The discrepancies in strength with a high risk priority number (245) suggest that, for products fabricated by additive manufacturing, a special care should be taken at the design stage. A high value of the risk priority number (210) also indicates that the strength properties are affected by the manufacturing process. This implies that corrective measures should be initiated with reference to the manufacturing process to reduce the value of the factor. The third important discrepancy concerns the measurement of strength properties (the risk priority number = 126). In this case, corrective measures should refer to the measurement uncertainty, which can be achieved by changing the measurement method or instruments, as well as increasing their precision. The risk priority number, being a measure of the innovation risk for additive manufacturing, indicates the severity of strength and possible problems related to it. Other discrepancies are less significant (the risk priority number < 100) and do not require any measures related to the innovation risk management.

## 6. Conclusions

From the analysis it is clear that Vero White, used to produce the specimens for static tensile tests, shows a clear anisotropy of the material properties with regard to the printing orientations. The same material was obtained for each of the printing directions; however, it differed in properties. The specimens with properties of a brittle material were produced when the object orientation on the build tray was vertical. The specimens showing the properties of a reinforced polymer with a clear yield point or with no yield point were obtained for the orientations in the Y and X directions, respectively.

Model materials obtained by additive manufacturing are not so well-known as metal alloys or plastics, the most common structural materials. It is thus essential to study them in detail

before they are commercially applied. The analysis results presented in this paper will be useful for designing models made of Vero White.

The paper has discussed the innovation risk associated with additive manufacturing. Of a particular importance are the mechanical properties of the materials. The analysis and assessment of measurement results should take into account risks to enhance the severity of the measurements and to provide design and process engineers with a knowledge that is useful when quality-related engineering decisions are taken with regard to the application of innovative solutions. Similarly, the use of the state-of-the-art measurement methods, discussed, for instance, in Ref. [25, 26], enhance the applicability of other innovative manufacturing processes. The FMEA method enables the detection and elimination of defects and errors as early as during the design and testing of innovative products, which, normally, would be detected during the product manufacture or use.

The risk analysis and assessment performed for the measurement data using the FMEA method indicate that products fabricated by additive manufacturing need to be applied with caution. Future research and development projects should aim to improve the manufacturing process, with attention to be paid to the strength properties of the materials. It is also very important to apply appropriate measurement techniques and instruments.

## Acknowledgements

The data presented in this paper are the results of the research supported by the ‘Regional Innovation System for the Świętokrzyski Province – Phase 4’ Project, WND – POKL.08.02.02 – 26 – 001/12 - Human Capital Operational Programme, Priority Axis VIII: Regional Human Resources of the Economy, Measure 8.2 Knowledge transfer, Submeasure 8.2.2 Regional Innovation Strategies.

The study was performed using the equipment purchased for *The Equipment Support for the Innovative Research Laboratories of the Kielce University of Technology (LABIN) Project* co-funded by the European Union within the Development of Eastern Europe Operational Programme 2007-2013, the Innovative Economy Priority Axis, Measure I.3: Support for Innovation.

## 7. References

- [1] Liu, H.C., Liu, L., Liu, N. (2013). Risk evaluation approaches in failure mode and effects analysis: A literature review. *Expert Systems with Applications*, 40, 828–838.
- [2] Su, X., Deng, Y., Mahadevan, S., Bao, Q. (2012). An improved method for risk evaluation in failure modes and effects analysis of aircraft engine rotor blades. *Engineering Failure Analysis*, 26, 164–174.
- [3] Kolich, M. (2014). Using failure mode and effects analysis to design a comfortable automotive driver seat. *Applied Ergonomics*, 45, 1087–1096.
- [4] Chen, P.-S., Wu, M.-T. (2013). A modified failure mode and effects analysis method for supplier selection problems in the supply chain risk environment: A case study. *Computers and Industrial Engineering*, 66, 634–642.
- [5] Wirandi, J., Alexander, A. (2006). Uncertainty and traceable calibration – how modern measurement concepts improve product quality in process industry. *Measurement*, 39, 612–620.
- [6] Hiller, J., Reindl, L. M. (2012). A computer simulation platform for the estimation of measurement uncertainties in dimensional X-ray computed tomography. *Measurement*, 45, 2166–2182.
- [7] Sen, M., Shan, H. S. (2005). Analysis of hole quality characteristics in the electro jet drilling process. *International Journal of Machine Tools & Manufacture*, 45, 1706–1716.
- [8] Asiltürk, I., Süleyman, Neseli S. (2012). Multi response optimisation of CNC turning parameters via Taguchi method-based response surface analysis. *Measurement*, 45, 785–794.

- [9] Campbell, I., Bourell, D., Gibson, I. (2012). Additive manufacturing: rapid prototyping comes of age. *Rapid Prototyping Journal*, 18, 4, 255–258.
- [10] Puebla, K., Arcaute, K., Quintana, R., Wicker, R.B. (2012). Effects of environmental conditions, aging, and build orientations on the mechanical properties of ASTM type I specimens manufactured via stereolithography. *Rapid Prototyping Journal*, 18, 5, 374–388.
- [11] Chockalingam, K., Jawahar, N., Chandrasekhar, U. (2006). Influence of layer thickness on mechanical properties in stereolithography. *Rapid Prototyping Journal*, 12, 2, 106–113.
- [12] Quintana, R., Puebla, K., Wicker, R.B. (2010). Effects of build orientation on tensile strength for stereolithography manufactured ASTM D-638 type I specimens of DSM Somosw 11120 resin. *Journal of Advanced Manufacturing Technology*, 46, 201–15.
- [13] Keşy, A., Kotliński, J. (2010). Mechanical properties of parts produced by using polymer jetting technology. *Archives of Civil and Mechanical Engineering*, X, 3, 37–50.
- [14] Hambali, R.H., Celik, H.K., Smith, P.C., Rennie, A.E.W., Ucar, M. (2010). Effect of Build Orientation on FDM Parts: A Case Study for Validation of Deformation Behaviour by FEA. *iDECON 2010 – International Conference on Design and Concurrent Engineering Universiti Teknikal Malaysia Melaka (UTeM)*, 224–228.
- [15] Radziszewski, L. (2004). Intrusive effect of a contact transducer on testing results, *Metrology and Measurement Systems*, XI, 1, 31–43.
- [16] Radziszewski L., Kekez M. (2009). Application of a genetic-fuzzy system to diesel engine pressure modeling. *The International Journal of Advanced Manufacturing Technology*, 46, 1-4, 1–9.
- [17] Cedro, L., Janecki D. (2011). Determining of Signal Derivatives in Identification Problems – FIR Differential Filters, *Acta Montanistica Slovaca*, R 16, cz. 1, 47–54.
- [18] ISO. Standard 527-1 (2012). Plastics - determination of tensile properties - Part 1: General principles.
- [19] Inspekt Mini (2011). Universal testing machine Inspekt mini 3kN. *Hegewald & Peschke MPT GmbH*.
- [20] LabMaster software (2011). Version 2.5.3.21.
- [21] Adamczak, S., Bochnia, J., Kaczmarek, B. (2014). Estimating the uncertainty of tensile strength measurement for a photocured material produced by additive manufacturing. *Metrology and Measurement Systems*, XXI, 3, 553–560.
- [22] Adamczak, S., Makiela, W. (2010). Fundamentals of metrology and quality engineering for mechanical engineers. *WNT*.
- [23] ISO. Standard 6892-1 (2009). Metallic materials – Tensile testing - Part 1: Method of test at room temperature.
- [24] Hamrol, A. (2005). Quality management with examples. *Wydawnictwo Naukowe PWN*. Warszawa, 327–336.
- [25] Stępień, K., Makiela, W. (2013). An analysis of deviations of cylindrical surfaces with the use of wavelet transform. *Metrology and Measurement Systems*, XX, 1, 139–158.
- [26] Janusiewicz, A., Adamczak, S., Makiela, W., Stępień, K. (2011). Determining the theoretical method error during an on-machine roundness measurement. *Measurement*, 44/9, 1761–1767.